LIGHTWEIGHT STIFFENED PANELS FABRICATED USING EMERGING FABRICATION TECHNOLOGIES: FATIGUE BEHAVIOUR

P.M.G.P. Moreira[1], V. Richter-Trummer[2], M. A. V. Figueiredo[2], P. M. S. T. de Castro[2]

[1] Instituto de Engenharia Mecânica e Gestão Industrial, INEGI-FEUP
Faculdade de Engenharia da Universidade do Porto,
Rua Dr. Roberto Frias, 4200-465 Porto, Portugal
E-mail: pmgpm@fe.up.pt

[2] Faculdade de Engenharia da Universidade do Porto and IDMEC-Porto
Rua Dr. Roberto Frias, 4200-465 Porto, Portugal
E-mail: ptcastro@fe.up.pt

ABSTRACT

The need for lower costs and the emergence of adequate welding technologies has brought interest in large integral metallic structures for aircraft applications; however, in integral structures, a crack approaching a stiffener propagates simultaneously in the skin and into the stiffener and breaks it. The use manufacturing techniques as high speed machining (HSM), laser beam welding (LBW) and friction stir welding (FSW) requires further experimental and numerical work concerning the fatigue behaviour of panels manufactured using those processes. A testing programme including fatigue crack growth rate characterization in panels fabricated using HSM, LBW and FSW was performed. Data obtained at IDMEC-Porto testing panels under R (min. load / max. load) of 0.1 and 0.5 is presented, and the performance of panels manufactured using the different processes is discussed and compared. The work was developed in the frame of the European Union DATON project.

KEY WORDS: Fatigue crack growth; Forman law; residual stress; stiffened panels.

1. Introduction.

Minimum weight is a major concern in aircraft design, [1]. Because of interest in integral structures, it has become increasingly important to develop methodologies to predict failure in fatigue damaged fuselage structures, [2], since the fuselage is supposed to sustain cracks safely until it is repaired or its economic service life has expired. Strength assessment of the structures is necessary for their in-service inspection, repair and health monitoring, [3]. Therefore, damage tolerance analysis should provide information about the effect of cracks on the strength of the structure. Recently, studies are being conducted to validate monolithic designs aiming at equal or better performance than conventional designs with regard to weight and structural integrity, while achieving a significant reduction in manufacturing cost, [4].

An aircraft fuselage structure includes, among other parts, the external skin and longitudinal stiffeners (stringers and longerons) [5]. Stiffened panels are light and highly resistant metal sheets reinforced by stringers structures designed to cope with a variety of loading conditions. Stiffeners improve the strength and stability of the structure and provide a means of slowing down or arresting the growth of cracks in the panel. Most common stiffener cross-sections are bulb, flat bar or T- and L-sections, that can be bonded, extruded, connected by means of fasteners, machined or welded to form a panel. When experimentally testing stiffened panels attention should be given to the loading and boundary conditions to ensure that the behaviour of the panel in the complete structure is reproduced, [6]].

The skin structure of a pressurized fuselage for transport aircraft is fatigue sensitive. The residual strength concept permits the determination of the maximum crack length that can be safely sustained. With this information and the characterization of the crack growth behaviour of the material, the number of loading cycles that will be necessary for the crack to grow up to its critical length can be estimated in order to ensure safe operation, [7]. The development of numerical methodologies with the help of small laboratory coupon test results should be used to predict the residual strength of complex built-up aircraft fuselage structures, [8].

Riveted and bolted stiffeners tend to remain intact as the crack propagates under them providing an alternative path for the panel load to pass. Also, riveted stiffeners continue to limit crack growth after the crack propagates past the stiffener since a crack cannot propagate directly into the stiffener. The permanent need for low cost and the emergence of new technologies has brought interest in large integral metallic structures for aircraft applications. Evaluative programs for replacement of

traditional fastening with these new emerging technologies have been carried out all over the aircraft sector, *e.g.* [9]. In an integral stiffener (machined, extruded or welded) a crack propagates simultaneously in the stiffener and in the skin beyond the stiffener. In this case the crack may propagate into and break the stiffener, [10], although in [11] it was observed that the rate of crack growth is significantly reduced in the skin in the presence of stiffeners.

There is an urgent pressure from the manufacturing side in the aerospace industry to apply advanced structural concepts, since they promise considerable cost and production time benefits, producing, in addition, a smaller number of fatigue and corrosion critical locations. The main drawback of integrally stiffened structures is the damage tolerance behaviour. Such design behaves totally different from the differential designs created by using riveted stiffeners. The prime problem is the crack arresting capability of the stiffeners both in fatigue crack growth as well as in residual strength

The first task in this study was the finite element method analysis of the stiffened panel geometry that was defined by the project guide lines.

2. Finite element analysis of the selected panel geometry.

The geometry of the specimen studied in the experimental component of the European Union DATON project [12] is presented in Figure 1. A three-dimensional (3D) stress analysis of the specimen was done using the finite element method (FEM) and ABAQUS [13].

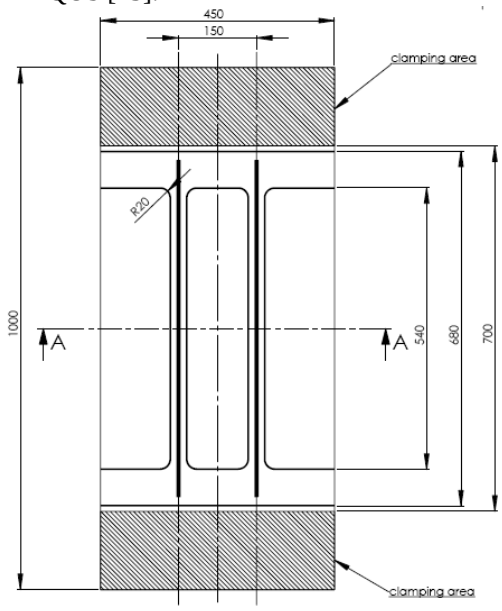

Figure 1 - Geometry of specimens to be used in the experimental component of the DATON project, [12].

The centre of gravity is located 2.76*mm* above the specimen front face. In all the analyses carried out the load was applied aligned with the centre of gravity. The remote load chosen for all analyses corresponds to a 100*MPa* uniformly distributed nominal stress. Three different situations were analysed: stiffened panel without and with a central crack, and stiffened panel with a central crack and an anti-bending device.

In the following analyses x (and 1) is the coordinate axis in the thickness direction, y (and 2) is the coordinate axis in the loading (longitudinal) direction, and z (and 3) is the coordinate axis in the transversal direction. The specimen side containing the stiffeners will be named back side, whereas the opposite side will be named front side.

8-nodes brick elements (C3D8) and 6-nodes brick elements (C3D6) were used to model the specimen. These elements use linear interpolation in each direction and are often called linear elements or first-order elements. A total of 60083 elements were used to model half of the stiffened panel.

The deformed 3D FEM model, that presents the stress in the load direction, σ_y throughout the un-cracked stiffened panel, is shown in Figure 2. In this figure, displacements were enlarged (deformation scale factor of 20) in post-processing of the FEM analysis.

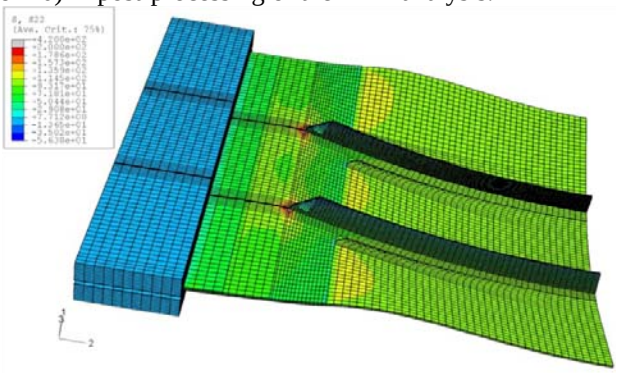

Figure 2 - Deformed model and stress distribution on the un-cracked stiffened plate, stress in the load direction.

A crack with length 2*a*=55.39*mm* was also modelled in the centre of the specimen. The detail of σ_y stress distribution in the cracked specimen middle cross section is presented in Figure 3. The σ_y stress distribution and displacements in the *x* direction were analysed along the nodes on the side of the plate containing the stiffeners and on the opposite side, in the direction of the arrow b) plotted in this figure.

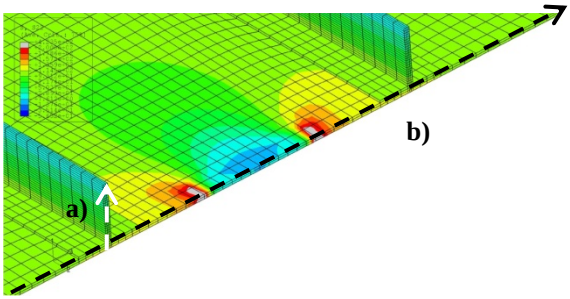

Figure 3 - Detail of specimen middle cross section, stiffened panel with a crack.

The evolution of σ_y stress along the nodes that lay on the arrow a), for the case of the un-cracked and cracked panels, is presented in Figure 4. For the un-cracked

panel, the stress values are higher in the plate and decrease through the stiffener moving away from the plate, as indicated by the arrow. The higher and lower σ_y stress values along this line are 112.2*MPa* and 17.5*MPa* respectively.
The introduction of a crack in the stiffened panel leads to an increase of the stress values in the plate and a decrease at the top of the stiffener.

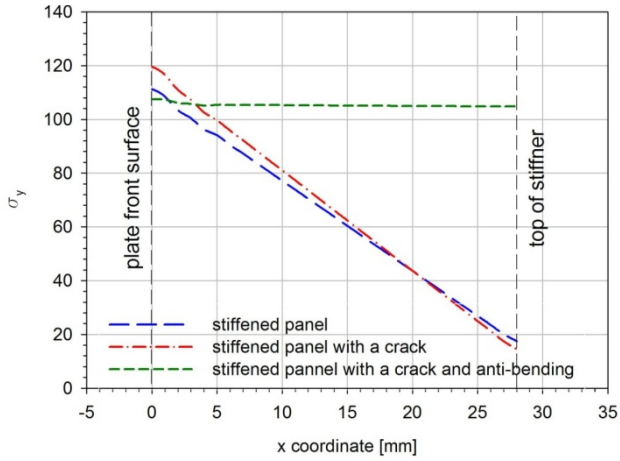

Figure 4 - Stress distribution along the nodes that lay on the arrow a) presented in Figure 3.

The σ_y stress distribution along the specimen longitudinal direction is presented in Figure 5. In this figure three lines - a), b) and c) – are marked. The σ_y stress and displacements in the x direction were determined along these lines. Results presented for lines b) and c) were obtained in the plate side opposite to the stiffeners (front side).

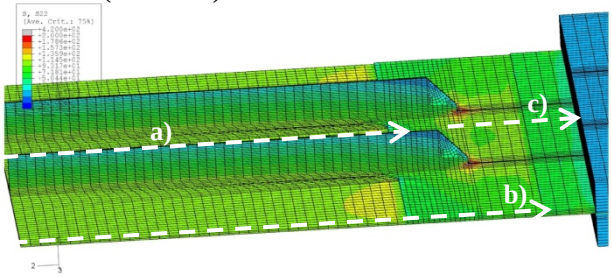

Figure 5 - σ_y distribution along the specimen longitudinal direction.

The σ_y stress distribution throughout the specimen longitudinal direction in the stiffener top surface a), panel lateral surface b) and panel longitudinal central line c) (as presented in Figure 5) is presented in Figure 6.
For the un-cracked panel, the higher stress values are found in the centre of the plate, but they are of the same magnitude as those found in the side layer. Stress values on the stiffener top surface are near 18*MPa*, except in the stiffener end where some low compressive values are found. When a crack is present there is a decrease of the σ_y stress value in the stiffener near the crack, but in the remaining stiffener σ_y stress has similar values as in the un-cracked panel. In the case of the cracked panel, σ_y stress is similar to the un-cracked panel, except in the middle plane near the crack face where σ_y has zero or very low values as expected.

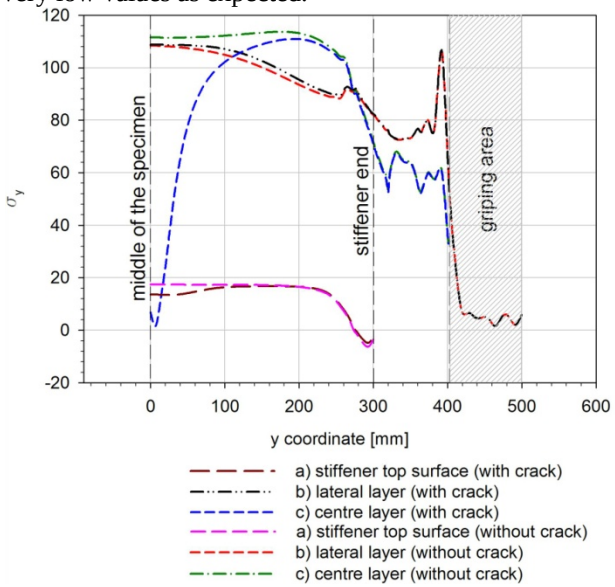

Figure 6 - σ_y distribution through the specimen longitudinal direction in stiffener top surface a), lateral surface b) and centre layer c), as presented in Figure 5. Stiffened panel with and without a crack.

3. DATON stiffened panels fatigue life; experimental measurements.

Fatigue tests of two stiffener specimens (Figure 1) manufactured by three different processes were carried out, HSM (High Speed Machining), LBW (Laser Beam Welding) and FSW (Friction Stir Welding). The stiffened panels were manufactured using the AA6056, a modified variant of the AA6013, which is considered a promising airframe candidate for processing by fusion laser beam welding and solid-state friction stir welding. The AA6056 is an Al-Mg-Si-Cu alloy that can be heat treated to different strength levels by precipitation hardening and has a good corrosion resistance. A total of ten specimens were tested.
Measurements of crack length in all specimens were performed according to the scheme presented in Figure 7. The specimen front and back sides are the sides of the plate side without and with stiffeners, respectively.

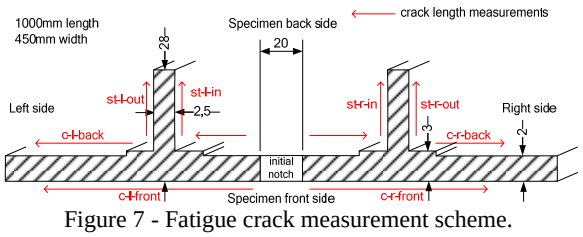

Figure 7 - Fatigue crack measurement scheme.

3.1 Base material tensile and crack growth tests.

Base material characterization was presented in [14]. It was verified that for both material conditions the specimens with R=0.5 presented a higher crack growth rate for the same ΔK value, as expected. Also, when tested at the same R value the specimens extracted from

the LBW panels have higher crack growth rate than those extracted from HSM panels.

3.2 High Speed Machining AA6056 panels.

Two stiffened HSM panels of aluminium 6056-T651 were fatigue tested at a maximum stress of 80*MPa* with *R*=0.1 (specimen HSM01) and at a maximum stress of 110*MPa* with *R*=0.5 (specimen HSM02). The stress distributing for static and fatigue loading was recorded and the crack growth rate was also measured. An initial central full depth notch (crack) with 20*mm* length and 0.2*mm* width was created by electro-discharge machining. In this paper, more complete details of the test procedure are given in the case of these HSM specimens. Testing of the remaining specimens, although also covering all aspects dealt with for HSM, is recorded here giving only the *a vs N* data, which was indeed the main testing objective.

Two panels with a central notch of 20*mm* length were instrumented and loaded at five incremental loads to acquire the stress distribution in specific sites of the specimen. The strain gages were distributed in the specimen according to the scheme presented in Figure 8: two couples (C1, C5, C6 and C7), on both faces of the panel, bonded on the skin at the centre of each bay (spaced 225*mm* in horizontal direction), on the horizontal symmetry plane; another couple (C3 and C8), placed on the longitudinal axis of the panel, 200*mm* above the horizontal symmetry plane; two couples (C2, C4, C7 and C9), placed in correspondence of a stringer, with a strain gauge bonded on top of the stringer and the other one on the skin.

An accurate symmetry of load distribution along the specimen width was identified. At the specimen horizontal middle line, the stiffener top surface has the lower values of stresses.

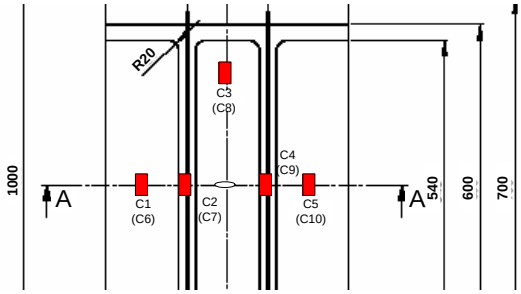

Figure 8 - DATON panel strain gages location (front gages in brackets, see Figure 7).

A value of 70*GPa* was used for the Young modulus in order to convert strain to stress.

Fatigue crack propagation tests were carried out and strain was measured in order to understand the different load transfer stages.

The strain gages values were measured in periodic stops of the fatigue test at the average fatigue load (44*MPa*, 47.98*kN*). The stress distribution on the stiffened panel along the fatigue test is presented in Figure 9. When the crack is near and reaches the stiffener most of the load is transmitted to the plate front side.

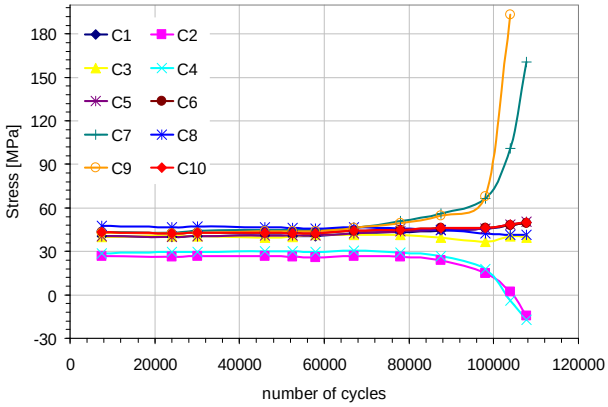

Figure 9 - Stress distribution during the fatigue crack growth test, HSM01 (σ_{max}=80MPa, *R*=0.1).

For specimen HSM02 (σ_{max}=110*MPa*, *R*=0.5) the strain gages values were measured in periodic stops of the fatigue test at the maximum fatigue load (119.95*kN*). Again, when the crack grows through the stiffener most of the load is carried out by the plate front side.

Fatigue crack propagation tests were carried out and crack length was measured at periodic stops of the fatigue test. Specimen HSM01, tested at a maximum stress of 80*MP*a and *R*=0.1, had a fatigue life of 113784 cycles. The fatigue crack growth in the stiffened panel during the fatigue test is presented in Figure 10. The first fatigue crack was only detected at 15000 cycles. The crack started to growth through the stiffener at 109800 cycles, 96.5% of the total fatigue life. The crack in the left stiffener bifurcated at nearly 113000 cycles.

Specimen HSM02, tested at a maximum stress of 110*MPa* and *R*=0.5, had a fatigue life of 117744 cycles. The first fatigue crack was first detected at 7500 cycles. The crack started to grow through the stiffener at 113000 cycles, 96.0% of the total fatigue life. After 115000 cycles the fatigue crack in both stiffeners bifurcated and started to propagate parallel to the panel along the stiffener.

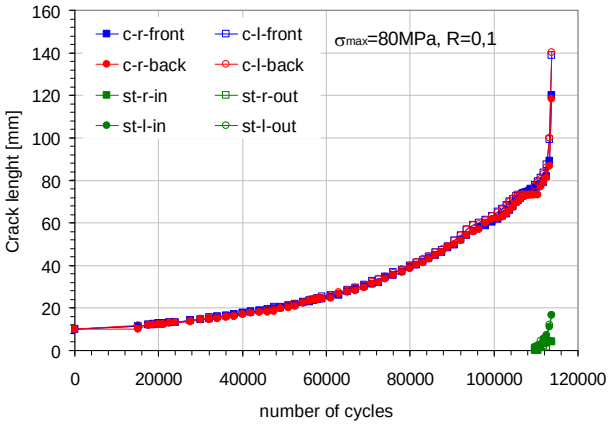

Figure 10 - Fatigue crack growth test, specimen HSM01.

3.3 Laser Beam Welded AA6056 2-stiffener panels.

Six laser beam welded panels of aluminium 6056 were fatigue tested. Half of the panels were tested at a maximum stress of 80*MPa* with R=0.1 and the

remaining at 110*MPa* and *R*=0.5. Panels with two different heat treatment conditions were tested:
i- after the welding procedure panels were submitted to an aging treatment T6 (PWHT) which corresponds to 4*h* at 190°*C*. The machining of the panels has performed on T4 tempered 5*mm* thickness sheet;
ii- another set of panels were previously heat treated to the condition T6 and than tested (as-welded).
Two different welding configurations were analyzed (LBW1 and LBW2), as presented in Figure 11. The main difference between LBW1 and LBW2 is the position of the weld bead. In the LBW1 configuration the weldment is at the junction of the skin with the blade (T-joint); in the LBW2 configuration the weldment is at the lower part of the stringer web (butt-joint), 1*mm* above the skin.

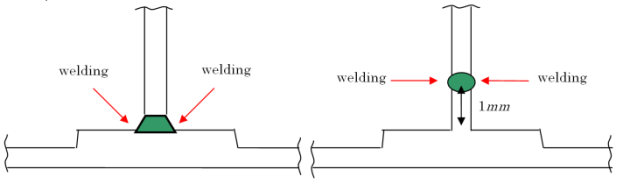

a) LBW1. T-joint b) LBW2. butt joint
Figure 11 - Welding configurations for the LBW specimens.

In subsequent sections of this paper, overall comparative plots of the data obtained for the remaining specimens will be given, and for the sake of concision no reference to specific features will be made.

3.4 Friction Stir Welding AA6056 2-stiffener panels.

Two stiffened friction stir welded panels of aluminium 6056 PWHT-T6 were fatigue tested: i) at a maximum stress of 80*MPa* with *R*=0.1; ii) and at a maximum stress of 110*MPa* with *R*=0.5. Panels were welded in the T4 condition, and after welding were tempered to achieve the T6 condition.

3.5 Results discussion

A comparison of the specimens tested with *R*=0.1 and *R*=0.5 (HSM, LBW1 PWHT-T6. LBW2 (as-welded and PWHT-T6) and FSW PWHT-T6) are presented in Figure 12 and Figure 13, respectively. For both values of *R*, the HSM specimen presented the lower fatigue lives. At the opposite, the PWHT-T6 specimens tested in the LBW2 configuration (butt joint) presented the higher fatigue lives for both *R* ratios.
The FSW specimen tested at *R*=0.1 presented a fatigue life similar to the LBW2 as-welded specimen. For *R*=0.5 the FSW specimen performed higher than the LBW1 PWHT-T6 specimen and lower than the LBW2 as-welded specimen.
In all specimens tested it was found that the crack arrest feature (decrease of crack growth rate) introduced by the stiffener was not significant, probably due to the low width of these specimens. Nevertheless when the stiffeners are fractured the remaining life of the specimen is marginal.
In a test of a multi-stiffener panel performed for AIRBUS [15] it was verified that there was a marked slow-down of crack growth rate as the crack reaches the stiffeners. However this phenomenon was not identified in the present tests of panels with two stiffeners. This difference can be attributed to the relatively light stiffeners used in the DATON panels when compared with the AIRBUS panel. These observations emphasise the need for further research studying the behaviour of stiffened panels with other ratios of stiffener to skin cross sections. Also, the number of stiffeners per panel, and the location of the initial crack (between stiffeners, or broken stiffeners) should be considered.

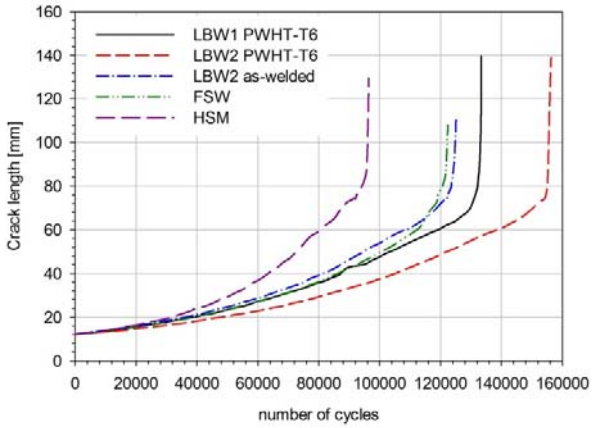

Figure 12 - Comparison of *a-N* for all specimens tested at *R*=0.1.

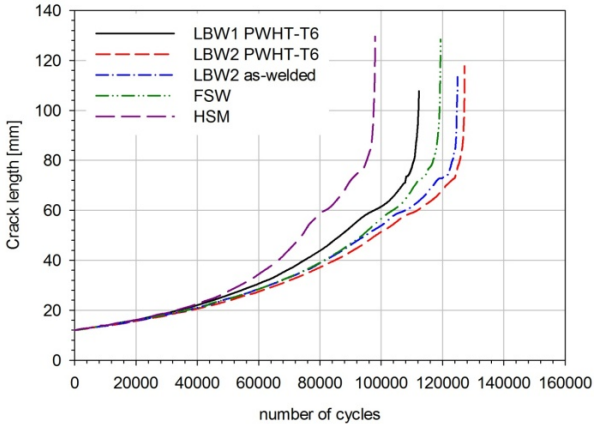

Figure 13 - Comparison of *a-N* for all specimens tested at *R*=0.5.

3.6 Crack growth prediction

Modeling of crack growth of HSM panels was carried out using the virtual crack closure technique (VCCT) for SIF calculation, ABAQUS finite element software and the Paris law with the constants mentioned earlier in the paper, [14]. Using an algorithm in MAPLE that integrates the Paris law equation and takes into account the SIF curve fit presented in [14], the number of cycles as a function of crack length was calculated and good agrement between experiments and model. The results of this modelling exercise were compared with the experimental measurements of the two HSM panels. The panels were tested at σ_{max}=80*MPa* *R*=0.1 and σ_{max}=110*MPa* *R*=0.5.
For both HSM specimens a good agreement between the predicted fatigue life and the experimental measurements was found. Once compared with panels

fabricated by welding, HSM panels are expected to present very low residual stress values. In the following discussion any machining residual stress were not taken into consideration. For the case of R=0.5 the predicted fatigue life was found to be slightly higher than the experimental measurements at a crack length a=60mm, and approximately 30% higher when critical crack length was reached. This difference can be due to the complex test setup used for experimental tests and to the simplified numerical model. It is to be noted that a difference of 20% in fatigue life is of the order of the scatter found when testing similar DATON panels under similar loading conditions, [16].

4. Conclusions

- The SIF calibration of the DATON panel was obtained using the VCCT technique in conjunction with a finite element model. The resulting SIF solutions for both skin and stiffener, used with the Paris law, gave adequate predictions of experimental crack propagation behaviour in HSM panels.
- When fatigue testing the DATON stiffened panels it was found that, although SIF decreases when cracks approach the stiffeners, there is no clear slowing down of the crack propagation.
- Welded panels presented longer lives up to rupture, implying that during most of their fatigue testing the crack growth rates were smaller than with HSM panels. This somewhat unexpected result is certainly associated to the residual stress fields existing in the welded panels, and also to the location of the initial artificial defect, placed in the skin precisely in the middle distance between the two stiffeners.
- In the LBW panels, at the centre of the weld, pores with a maximum diameter of approximately 0.24mm were identified. These pores seem to be coincident with the laser maximum penetration depth from each side of the T-joint. In the transition area between the melted and un-melted material cracks out of the weld bead were identified.
- In the FSW panels it is verified that outside the weld affected area the fracture shows a more regular structure than in the weld affected area. This difference was reflected in the striation identification process; it was harder to perform the analysis under the shoulder limits. In the thermomechanically affected zone, inside the stiffener, a change in the fracture surface occurs.

References

1. J. Paik, S. van der Veen, A. Duran, and M. Collette, *Ultimate compressive strength design methods of aluminum welded stiffened panel structures for aerospace, marine and land-based applications: A benchmark study.* Thin-Walled Structures, 2005. **43**(10): p. 1550-1566.
2. P. Wen, M. Aliabadi, and A. Young, *Fracture mechanics analysis of curved stiffened panels using BEM.* International Journal of Solids and Structures, 2003. **40**(1): p. 219-236.
3. A. Murthy, G. Palani, and N. Iyer, *Remaining life prediction of cracked stiffened panels under constant and variable amplitude loading.* International Journal of Fatigue, 2007. **29**(6): p. 1125-1139.
4. R. Pettit, J. Wang, and C. Toh, *Validated feasibility study of integrally stiffened metallic fuselage panels for reducing manufacturing costs*, in *NASA / CR-2000-209342*. 2000.
5. A. Murphy, M. Price, C. Lynch, and A. Gibson, *The computational post-buckling analysis of fuselage stiffened panels loaded in shear.* Thin-Walled Structures, 2005. **43**(9): p. 1455-1474.
6. A. Aalberg, M. Langseth, and P. Larsen, *Stiffened aluminium panels subjected to axial compression.* Thin-Walled Structures, 2001. **39**(10): p. 861-885.
7. N. Salgado and M. Aliabadi, *The application of the dual boundary element method to the analysis of cracked stiffened panels.* Engineering Fracture Mechanics, 1996. **54**(1): p. 91-105.
8. B. Seshadri, J. Newman, and D. Dawicke, *Residual strength analyses of stiffened and unstiffened panels - Part II: wide panels.* Engineering Fracture Mechanics, 2003. **70**(3-4): p. 509-524.
9. E. Hoffman, R. Harley, J. Wagner, D. Jegley, R. Pecquet, C. Blum, and W. Arbegast, *Compression buckling behavior of large-scale friction stir welded and riveted 2090-T83 A1-Li alloy skin-stiffener panels*, in *NASA/TM-2002-211770*. 2002.
10. H. Mahmoud and R. Dexter, *Propagation rate of large cracks in stiffened panels under tension loading.* Marine Structures, 2005. **18**(3): p. 265-288.
11. S. Mellings, J. Baynham, R. Adey, and T. Curtin, *Durability prediction using automatic crack growth simulation in stiffened panel structures*, in *http://www.beasy.com/*. 2002.
12. DaToN, *Innovative Fatigue and Damage Tolerance Methods for the Application of New Structural Concepts*. Strengthening the competitiveness, Specific Targeted Research Project. 2004: A Proposal for the 6th European Framework Program.
13. Hibbitt, Karlsson, and Sorenson, *ABAQUS Users Manual*. 2006.
14. P. M. G. P. Moreira, V. Richter-Trummer, S. M. O. Tavares, and P. M. S. T. de Castro, *Characterization of fatigue crack growth rate of AA6056 T651 and T6: Application to predict fatigue behaviour of stiffened panels. Materials Science Forum*, 2010. **636-637**: p. 1511-1517.
15. R. Franke, B. Brenner, V. Ulbricht, and W. Zink. *Moderne werkstoffe und testmethoden in flugzeugbau.* in *Tagungsband zum 6. Chemnitzer Symposium Fugetechnik/Schweisstechnik*. 2004. Technische Universitat Chemnitz.
16. University of Pisa, *WP3: Manufacturing and testing, Status at month 30.* DaToN project, meeting at Brno, slides presentation, 15-16 October 2007.